Annals of Ecology and Environmental Science
Volume 3, Issue 2, 2019, PP 37-49
ISSN 2637-5338

The Use of Interferometric Coherence of Sentinel-1a Images to Study Silting in South-East Morocco

Mohamed ABBA[1*], Ali ESSAHLAOUI[1], Omar ELKHARKI[2], Jamila MECHBOUH[3]

[1]Equipe de Recherche en Sciences de l'eau et ingénierie de l'environnement, Département de Géologie, Faculté des Sciences, Meknès ; B.P 11201 Zitoune Meknès, 50000 Maroc.
[2]Filière Ingénieur GéoInformation, Faculté des Sciences et Techniques, Tanger, Maroc.
[3] RIFGéomatique, Tanger Maroc.

***Corresponding Author:** Mohamed ABBA, Equipe de Recherche en Sciences de l'eau et ingénierie de l'environnement, Département de Géologie, Faculté des Sciences, Meknès ; B.P 11201 Zitoune Meknès, 50000 Maroc. Email: ouassimabba@gmail.com*

ABSTRACT

South-East of Morocco is threatened by active dunes; this is due to the scarcity of soil cover due to the combined effects of drought and anthropogenic actions. Terrain Observation by Progressive Scans (TOPS) mode from the Sentinel-1 satellite provides us with up-to-date high-quality Synthetic Aperture Radar (SAR) images over a wide ground coverage (250 × 250 km), enabling full exploitation of various In SAR applications. The SAR (Synthetic Aperture Radar) Interferometric Coherence Information provides an original measure of the dynamics and surface changes that occur between two SAR acquisitions.

In this study, Sentinel-1 TOPS data were employed to investigate dunes activities and silting. The Sentinel-1A mission allows the acquisition of radar images at 12 days apart. Thanks to this temporal base, the images of interferometric coherence combined with the amplitude images made it possible to detect the active sand zones as well as the areas of Ossian vegetation. In this paper we used four images SAR sentinel-1A in SLC mode (Single Look Complex) were acquired with 12 days interval on the study area: two in May 2015 and the other two in November 2017. The temporal analysis of the images of coherence was able to highlight the extension of the active sandy areas over time and the migration of the dunes. Interferometric coherence therefore seems to be a very good tool for mapping dune activity, as well as for tracking dune movements and silting.

The results illustrate the potential of interferometric coherence images as a useful source of information for the detection of sand dune movements in semi-arid zones.

***Keywords:** Radar interferometer, Sentinel-1A images, coherence, dune migration, silting.*

INTRODUCTION

The SAR Radar Image is a high-resolution image obtained from a synthetic aperture radar. The image in SLC mode (Single Look Complex) is a complex image with amplitude information and phase information from the backscatter signal. The amplitude depends on the reflectivity and geometry of the surface, as well as the roughness and physico-chemical nature of the targets that make up the pixel on the ground. The phase contains two terms: one is relative to the optical path travelled by the radar wave between the sensor and the target, it is the transport phase of the signal. The other is backscatter: it is the reconstruction phase resulting from the responses of each of the elementary backscatters within the pixel under consideration.

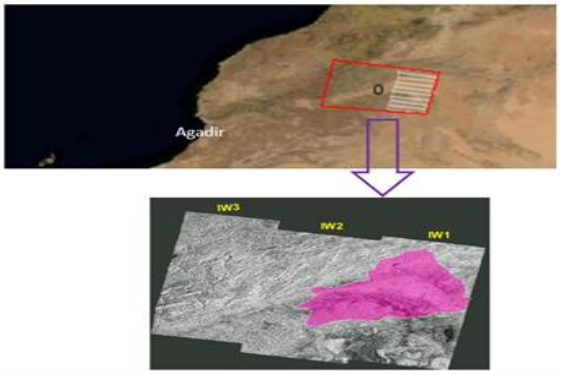

Figure1. *Location of Study Area (Colored Area) and Sentinel-1A Image*

The Differential interferometry (DInSAR) is a powerful tool for detecting and monitoring soil deformations on the one hand and generating the digital terrain model on the other. The objective

of this work is to track surface dynamics (movement of sandy) between two dates from two sentinel-1A radar images in SLC mode by exploiting interferometric coherence.

Figure 1 shows the geographic location of the study area and the Sentinel-1A image.

S-1 employs three predefined subswathsin IW mode (IW1, IW2, and IW3), achieving a ground swath coverage of 250 km in the across-track direction.

DATA USED

The Sentinel-1A Satellite

Sentinel-1A, a space mission of the Europe Space Agency of the Copernicus Programme, was launched on 3 April 2014. This mission provides C-band continuity following the retirement of ERS-2 and the end of the Envis at mission (ESA, 2016).

Compared to other SAR missions, his short revisit time (twelve days alone, and six days with Sentinel-1B) and short baselines (i.e. orbital separations) make Sentinel-1A promising in terms of In SAR applications.

Its new type of Scan SAR mode, known as TOPS SAR, has a similar pixel resolution (about 3.5 m in the range direction and 14 m in the azimuth direction) to Scan SAR but with an enhanced signal-to-noise ratio distribution (Farkas et al., 2015; Hervé Rivano, 2014).

Table1. *Detailed parameters of the Sentinel-1 data.*

Parameter	Value
Azimuth angle	−9.7 (degrees)
Incidence angle	43.9 (degrees)
Pixel spacing in slant range	2.3 (m)
Pixel spacing in azimuth	13.9 (m)
Wavelength	5.6 (cm)

The Modes of Acquisition of Sentinel-1A Images

The Sentinel-1 Operates in Four Exclusive Acquisition Modes

Strip Map (SM): in strip map mode, the instrument provides uninterrupted coverage with a geometric resolution of 5 m by 5 m at a swath width of 80 km. Six overlapping swaths cover a range of 375 km. For each swath, the antenna is configured to generate a beam with fixed azimuth and elevation pointing. Elevation beam forming is applied to suppress range ambiguity. Strip map mode will only be operated on request for extraordinary situations.

This mode offers data products in a single polarization (HH or VV) or in double polarization (HH + HV or VV + VH).

Interferometric wide Swath (IW): this mode implements a new type of Scan SAR mode called Terrain Observation with Progressive Scan (TOPS) SAR aimed at reducing the drawbacks of the Scan SAR mode. The basic principle of TOPSAR is the shrinking of the azimuth antenna pattern (along track direction) as seen by a spot target on the ground. This is obtained by steering the antenna in the opposite direction as for Spotlight support.

TOPSAR mode aims to achieve the same coverage and resolution as Scan SAR, but with a nearly uniform Signal-to-Noise Ratio (SNR) and Distributed Target Ambiguity Ratio (DTAR). TOPS employ a rotation of the antenna in the azimuth direction. Similar to Scan SAR, several sub-swaths are acquired quasi-simultaneously by sub-swath switching from burst to burst. The increased swath coverage is achieved by a reduced azimuth resolution, as in Scan SAR. However, in TOPS the resolution reduction is obtained by shrinking virtually the effective antenna footprint to an on-ground target, rather than slicing the antenna pattern, as happens for Scan SAR.

This mode offers data products in a single polarization (HH or VV) or in double polarization (HH + HV or VV + VH).

Extra Wide Swath (EW): This acquisition mode operates in a spatial resolution of 25m / 100m.

Wave (WV) Mode: has a resolution of 5 meters by 20 meters and a low data rate. It produces images of 20 km by 20 km along the orbit at intervals of 100 km.

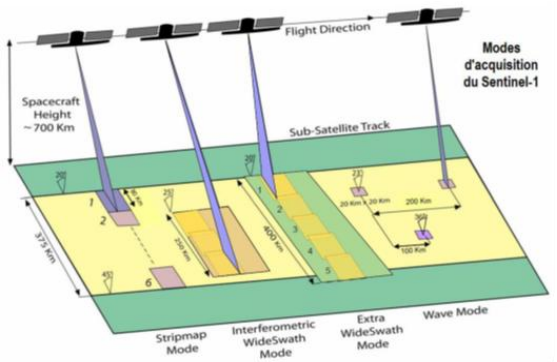

Figure2. *Sentinel-1 Acquisition modes (ESA, 2007)*

The TOPS SAR acquisition mode is capable of providing wide range swaths as with the Scan SAR technique, but it almost eliminates the

associated problems of scalloping and azimuth varying signal-to-noise ratio, noise equivalent sigma zero, and azimuth ambiguities (De Zan F. and Monti Guarnieri A. 2006).

In addition to scanning in elevation in order to extend the range coverage, the antenna azimuth beam is steered electronically from aft to fore at a constant rate. The scan pattern is shown in Fig. 3. As a result and in contrary to Scan SAR, all targets on the ground are observed by the entire azimuth antenna pattern. The acquisition takes place by recording bursts of echoes, i.e., employing sub apertures, at the expense of a lower azimuth resolution. S-1 employs three predefined sub swathsin IW mode (IW1, IW2, and IW3), achieving a ground swath coverage of 250 km in the across-track direction.

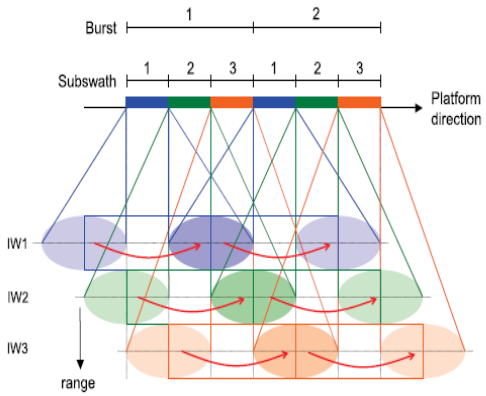

Figure3. *TOPS Scan pattern for S-1 IW mode, composed of three sub swaths.*

The SENTINEL-1 C-SAR system is designed to enable TOPS burst synchronization of repeat pass data takes supporting the generation of TOPS interferograms and coherence maps. Specifically, for the IW and EW modes, the TOPS burst duration is 0.82 s and 0.54 s (worst case) respectively, with a requirement for achieving a synchronization of less than 5 ms between corresponding bursts. TOPSAR requires high accuracy for image co-registration. A small co-registration error in azimuth can introduce an azimuth phase ramp due to the SAR antenna azimuth beam sweeping causing Doppler centroid frequency variations of 5.5 kHz.

This mode has a spatial resolution of 5m/20m and ground swath coverage of 250 km. IW is the main operating mode on earth. IW accomplishes interferometry through synchronization of bursts. The acquisition starts with the first burst of the first subswath (blue) at top left with the beam steered along azimuth in the same direction as the platform moves(as depicted by the red arrows). Once this burst has been acquired, the antenna is switched in elevation, and the first burst of the second subswath (green) is acquired. Once the first of the third subswath (orange) is acquired, the beam is switched back to the first subswath, and the process is cyclically repeated.(Nestor Yague Martinez et al. 2016).

Principle of Interferometry

The SAR Interferometry (INSAR) consists of interfering with two SAR images of the same region, which were acquired from two slightly different positions in space or time (Fig.4). When a target is viewed from two slightly different angles, the elevation of the target can be accurately recovered using phase information, which allows for a 3-dimensionalreconstruction of the observed scene (El kharki et al., 2016).

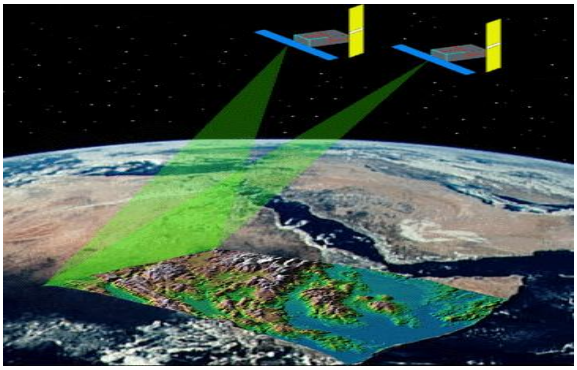

Figure4. *Acquisition of two images from two satellite passages (two adjacent orbits)*

The distance between the two satellites (or orbits) in the plane perpendicular to the orbit is called the interferometer baseline (see Figure 5) and its projection perpendicular to the slant range is the perpendicular baseline. The time base is the time interval between the two acquisitions.

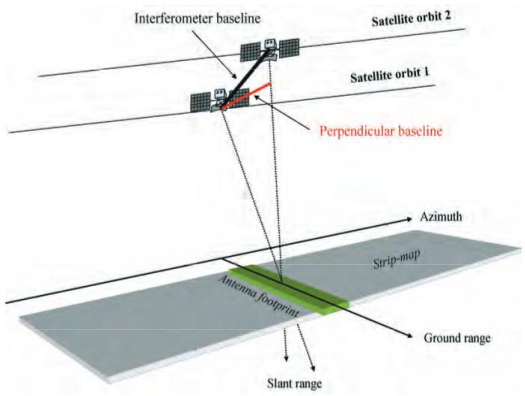

Figure5. *Geometry of a satellite interferometric SAR system. (Alessandro F. and al. 2007).*

The SAR interferogram is generated by cross-multiplying, pixel by pixel, the first SAR image with the complex conjugate of the second.

The radar beam emitted by the antenna is backscatters in all the directions by targets on the ground. Thus a more or less important part of the signal returns towards the satellite. The radar antenna crosses then in mode reception and measures the amplitude of the received signal but also its phase. Thus every radar pixel contains two information:

- Information of amplitude, which depends on characteristics of backscatter (properties geometry, dielectric properties) elementary targets contained in the radar pixel.
- An information of phase, which corresponds to the phase shift enters the radar backscattered wave and the wave of reference generated by the clock of the satellite.
- The recorded phase is the sum of two contributions:

$$\varphi = \varphi_{géom} + \varphi_{prop}$$

- The phase of (geometrical) route which depends time which put the wave to travel the return route between the satellite and the ground,
- The pixellar phase which corresponds to the phase signature of the pixel (internal contribution).It is related to the dielectric and geometric properties of the target.

Image of Coherence

Coherence is determined by the difference between the phases of reconstruction from one image to another, which is itself generated by a difference in the relative distribution of elementary targets or a change in dielectric properties within a pixel. The image of coherence is seen in a way as an image of the degree of confidence to be attributed to the interferogram. It contains information on the internal stability of the surface and estimated according to the following equation:

$$\rho = \frac{\left|\left\langle z_1 z_2^* \right\rangle\right|}{\sqrt{\left\langle z_1 z_1^* \right\rangle \left\langle z_2 z_2^* \right\rangle}} \qquad 0 \le \rho \le 1$$

Then we define for a given pixel the coherence from the two complex values Z1 and Z2 (master S1 and slave S2).

This is an indicator to show the variation in backscatter characteristics. As such, coherence is both an indicator of interferometric phase quality and changes in soil surface characteristics. If the objective of the interferometric measurement is the deformation of the surface of the soil, low orbital differentials and possible low acquisition times will be preferred, but especially compatible with the deformation to be measured. Loss of coherence determines the variance of the phase signal. But coherence is also a valuable and unique source of information that informs us about the surface and volume processes appearing between the two passages of the satellite and affecting the stability of the scene at the wavelength scale. It can be used as a pseudo-channel during classifications or as a change detection index. Coherence from ERS 1 and 2 images has been used by various works to detect and classify vegetation or moisture change (Santoro et al. 2007). Other authors have also tested the use of interferometric coherence for mapping sandy areas (Liu et al. 2001; Bodart et al. 2010).

The values of coherence vary between 0 and 1. When the consistency is equal to 1, the two images are perfectly consistent (complete absence of noise, the elementary targets inside a pixel contribute in the same way in each of the two images).However, when it is zero, the signals are completely decorrelated, there is no interference (the interferometric phase is totally noisy).
The relative position of targets within the pixel can be altered by different factors, which are all possible sources of decorrelation. By generalizing, coherence can be expressed through the product of these different sources (ESA 2016).

$$\gamma \text{ totale} = \gamma \text{ temporelle} \times \gamma \text{ spatiale} \times \gamma \text{ volumique} \times \gamma \text{ thermique} \qquad (1)$$

The contribution of decorrelation sources

This distinguishes temporal decorrelation γ, which is due to real changes in targets, other changes induced by the sensor and its geometry such as spatial decorrelation γ and thermal noise γ, which is due to system characteristics and

changes induced by vegetation (volume backscatter).

The spatial or geometric decorrelation is induced by the geometry of the shooting and the change in angle of incidence between the two shootings. This change in angle of impact induces a change in the relative positions of scatterers within the same pixel. Even in the absence of any other change, scatterers therefore do not identically give the same phase response between one and the other acquisition. So, there is a lack of coherence. For a flat soil, this decorrelation can thus be expressed in terms of a perpendicular base. As indicated in the following formula (Equation 2), the larger the base, there is less coherence (Zebker et Villasenor 1992)

$$\gamma_{spatiale} = 1 - \frac{2|B|R_y \cos^2\theta}{\lambda r} \quad (2)$$

where Ry is the ground resolution in the direction of the range, θ the viewing angle in the center of the swept band, r the distance of the sensor in the center of a pixel and λ the wavelength of the radar.

The loss of coherence can be a change in soil moisture or vegetation cover, a change in surface roughness such as falling leaves of trees, plant growth, wind blast in leaves or water, rain or snowfall… In short, any change at the wavelength scale that may result in changes in relative sprinkler positions within the pixel or changes in electrical characteristics. S and movement could therefore be one of these physical parameters responsible for the loss of coherence between two images. Only rocky or urbanized areas without vegetation retain their stability even over several years (high coherence).On the other hand, forests or bodies of water often show very little coherence even on a day of interval.

METHODOLOGY

To track silting using interferometric coherence, we selected four Sentinel-1A images, two May 2015 SLC images (03 and 15 May 2015), and two others SLC images dated 12 November 2017 and 24 November 2017 respectively. We chose images that are taken in different seasons (Humid and Dry) because we were careful to determine the impact of climate change on land use in general and particularly on silting, which could lead to comparable results. First, we visualize the images using the SNAP software with the determination of the characteristics of the selected SLC images. Then, we performed a TOPS SAR processing of the images by selecting the IWs that correspond to our study area (Fig. 1).In Figure 4, we show a diagram that summarizes the sequence of the treatments we performed on the Sentinel-1A images.

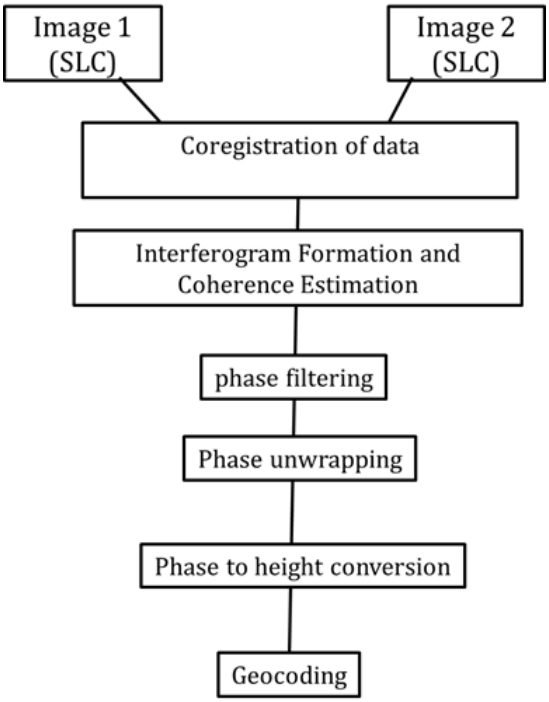

Figure4. *Sentinel-1 TOPS interferometric processing chain*

All the Sentinel-1images used were acquired in IW_SLC mode with a double polarization VH and VV.

Table1. *Characteristics of Sentinel-1 images used*

Parameters	Characteristics
Mission	Sentinel_1A
Polarization	VH et VV
Range spacing	2.33 m
Azimuth Spacing	13.95 m
Mode of acquisition	IW (Interferometricwide)
Antenna pointing	Right
Pass	Descending
Track	81

SENTINEL-1 TOPS INTERFEROMETRIC PROCESSING CHAIN

The Sentinel-1_IW_ SLC product can be acquired from the ESA's Sentinel Scientific Data Hub website. This product includes three subswaths ("burst SLC") which are obtained by processing the bursts over it. As shown in Figure. 5, the whole SLC is covered by several bursts and the overlaps appear in individual bursts in both azimuth (between sub-sequent bursts) and range (between neighboring sub-

swaths).The first step in the SLC processing chain is the separation of the three Radar imaging sub-swaths using the SNAP Software operator S1-TOPSAR:

- TOPSAR split: each image is divided into three sub-swaths (Fig 5)
- TOPSAR Deburst: Debursting is the elimination of horizontal black bands, known as burst, on each subswath (Fig 6). and TOPSAR Merge: an operation that merges the three subswath to obtain a complete interferogram (Fig7).

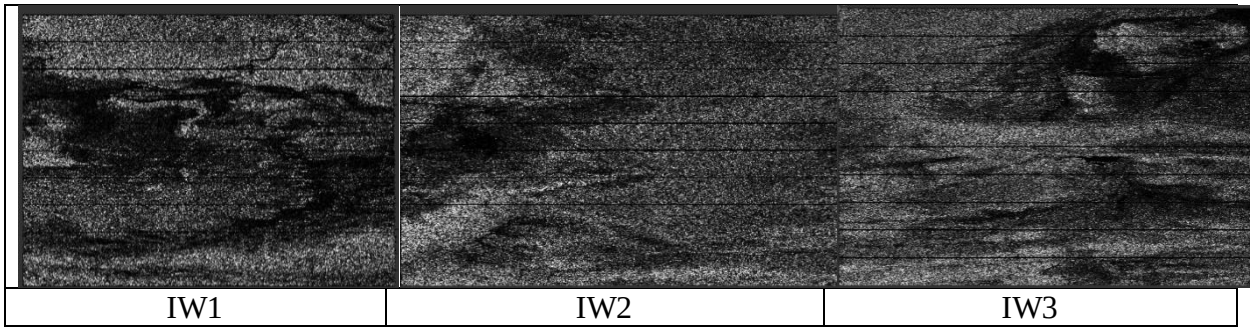

Figure5. *Three subswaths ("burst SLC")*

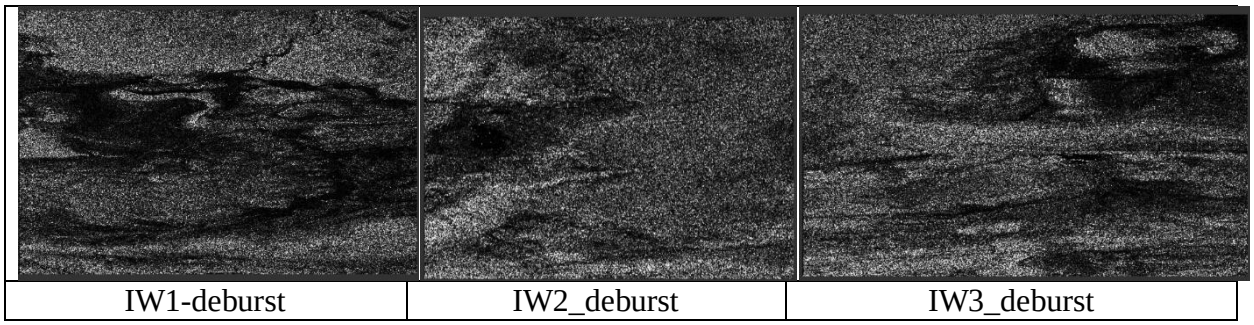

Figure6. *IW sub-swath without demarcation lines (Debursts)*

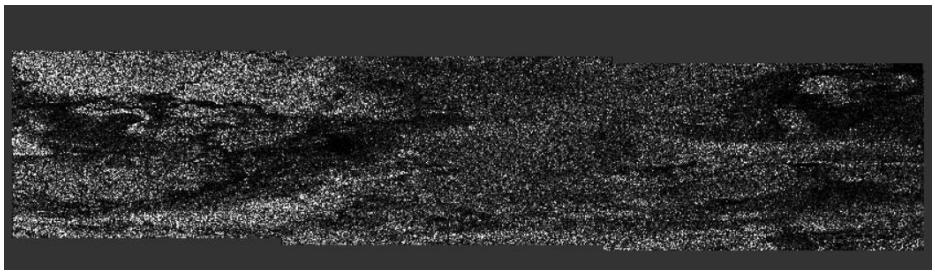

Figure7. *Sentinel-1A image of May 03, 2015*

Radiometric Calibration

Each pixel of a radar image is defined by a digital account (CN). This numeric account depends on the acquisition parameters. It is therefore difficult to compare it from one image to another. In order to perform multi-temporal analysis and compare different images, it is necessary to standardize the signal intensity. This standardization is ensured by the radiometric calibration of the images. To compare two images taken during different acquisitions, it is necessary to compare values representative of the ground, independent of the acquisition conditions (due to the sensor).An example of this type of value, known as quantitative, is called sigma_0, or backscatter; value that can be given in natural value or converted to dB (decibel). To transform the predefined values in the Sentinel images into this value, the process is called calibration. The operation consists of the application of a formula (known by the software) dependent on the image acquisition sensor.

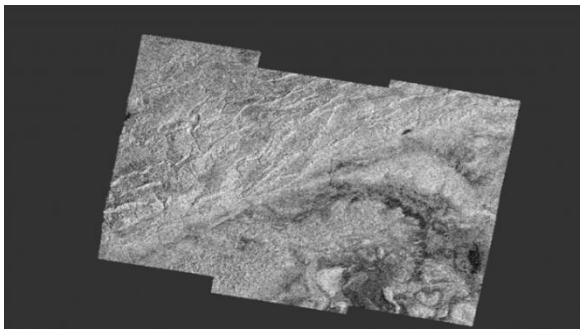

Figure8. *Sigma-0_VV image (May 03, 2015)*

Coregistration

The principle of the interferometry is based on the exploitation of two radar images. These images correspond to shots of the ground since rather close satellite positions. They are slightly deformed the one with regard to the other one. This requires treatment in order to place them in a common geometry so that they are stackable, in a way that two identical pixels in both images represent the same element on the ground. One of the two images will be called chief "image". By opposition, the other image will be taken as "embellishes with images slave". The geometry of shooting of the chief image will be considered reference. The type of geometrical processing to flush the two images of the same scene in order to manipulate them in the same geometry (master image geometry) is called coregistration.

Coregistration consists in determining the position of the pixels of the slave image considered to be mobile, according to the natural coordinates of the master image considered to be fixed. This technique conditions the quality of the data and their exact interpretation. It can be used differently depending on the nature of the initial data.

Interferogram Training and Coherence Estimation

After making the two images stackable by the recalibration process, the interferogram is generated. The latter is the result of the difference in the phase of the master image and the slave image and is presented as an interference image, containing fringes equivalent to curves of levels at the different values of the phase difference. The generation of the interferogram consists simply in multiplying point to point the complex value of each pixel of the master image by the complex conjugated with the corresponding pixel value in the slave image.

The time gap between the two images is 12 days (which corresponds to the period of revolution of the S-1A satellite).After coregistration, the phase difference ϕ is calculated point by point between the two images, this phase difference modulo 2π gives rise to an interference image called an interferogram that contains fringes equivalent to level curves and sensitive to changes in Height of ground. Several physical phenomena can occur together in the production of phase difference fringes in the interferogram.

$$\Delta\varphi = \Delta\varphi_{orb} + \Delta\varphi_{atm} + \Delta\varphi_{topo} + \Delta\varphi_{dep} + \Delta\varphi_{br} + 2k\pi$$

Equation of different contributions in the SAR interferometric phase difference

φ : phase difference

φOrb : Orbital phase difference (flat terrain).It is due to the curvature of the earth

φ atm: phase difference due to changing atmospheric conditions

φ topo: phase difference from topography geometry.

φ Dep: phase difference related to ground displacement, measured by line of sight.

φ noise: residual phase difference (noise) from treatments (coregistration, SAR recording).

Through interferometric treatment, we will try to eliminate sources of error to leave only the contribution of interest that is usually elevation or displacement. Radar interferometry uses phase information contained in radar images as a means of measuring distance. Analyzing transients between two complex images acquired under neighboring geometrical conditions. Unfortunately this phase information is taken modulo 2π, it means that we do not distinguish the actual elevations (altitudes) from the reliefs corresponding to phases having the same remainder of the division by 2π, in order to determine this actual elevation, we use the phase sequence technique to rebuild the topographic image from that of the interferometric phase.

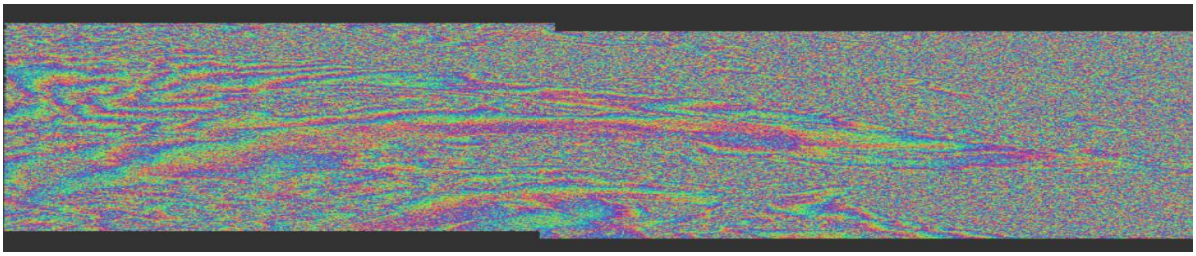

Figure9. *Interferogram of May 2015 (Unwrapped phase)*

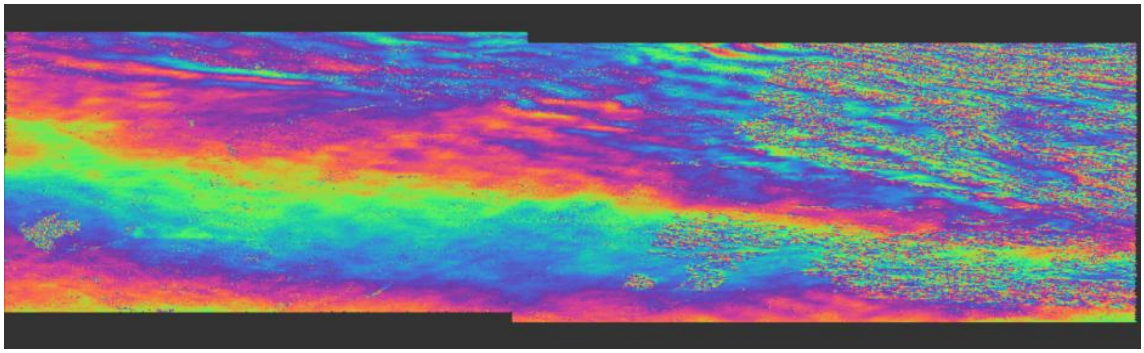

Figure10. *Wrrapped phase of May 2015*

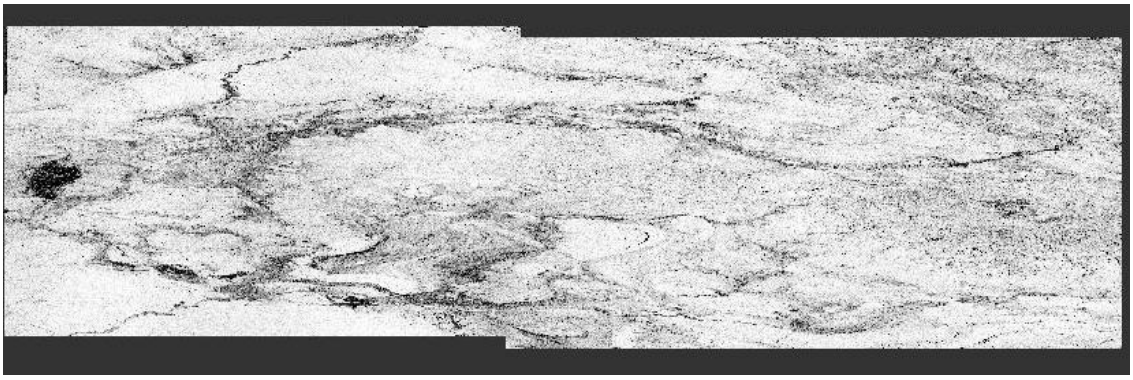

Figure11. *Coherence image of November 2017*

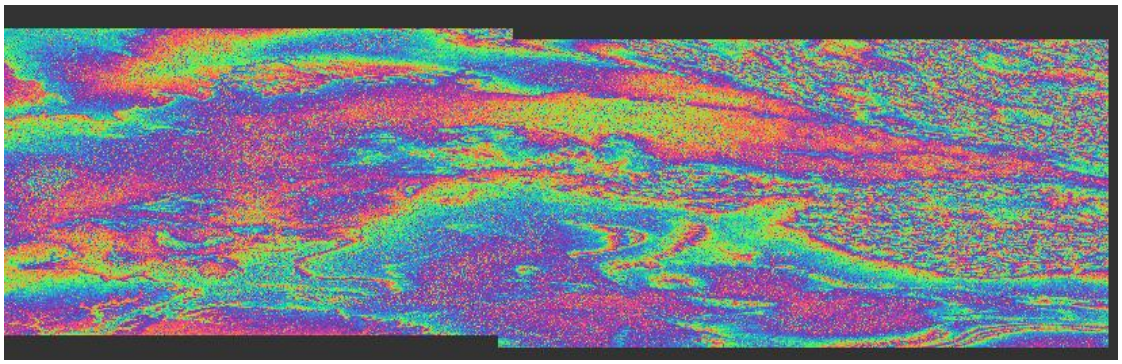

Figure12. *Interferogram of November 2017*

RESULTS AND INTERPRETATIONS

Image of Coherence

The interferometric coherence is defined as a complex crossed correlation between both images: master and slave. The band of coherence (fig12) shows how every pixel is similar between the images slave and master in a scale from 0 to 1.The zones of strong coherence (close to 1) seem brilliant. Zones with low coherence (close to zero) will be dark. The dark zones on the image of coherence above correspond to the pixels where the signals are completely uncorrelated, there is no interference (the interferometric phase is totally noisy), Loss of coherence in our study area could be caused by three distinct aspects:

- A change in the roughness of the vegetation surface (palm grove area) such as falling leaves of trees, plant growth, blowing wind in leaves.
- A change in the roughness of the water surface such as the wind blast on the water (Hassan Addakhil Dam).
- A change due to the movement of sand could therefore be one of these physical parameters responsible for the loss of coherence between two images.

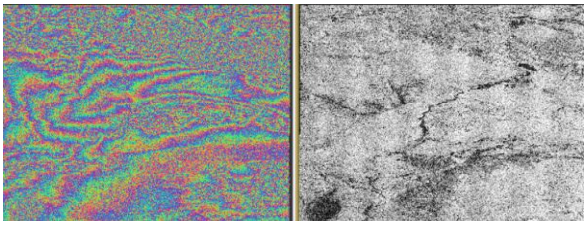

Figure13. *Phase band (left) and coherence band (right) not corrected*

The interferometric phase can be used to:

- Generate the topography
- Measure ground movements

The phase difference used in interferometry requires a sufficient correlation between the data acquired by the satellite during the observation cycles. Decorrelation is the result of several phenomena that disrupt the phase difference between the two images.

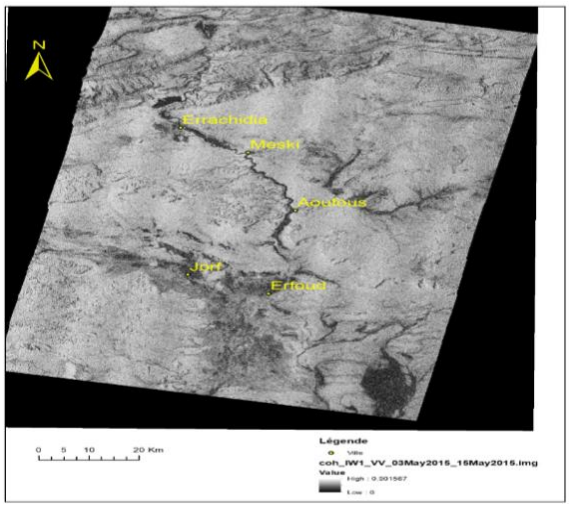

Figure14. *Coherence of Sentinel-1A_IW1 image acquired in May 2015 after geo referencing*

This decorrelation manifests itself in the form of a visible noise in the interferogram and a drop in the measured consistency. It means a change in the observation geometry or the apparent relative position of the backscatters. The image of coherence is seen in a way as an image of the

degree of confidence to be attributed to the interferogram. It contains information on the internal stability of the surface. Forests have lower coherence because of a faster change in vegetation cover and a possible backscatter density. On the other hand, plains, towns and artificial structures show little variation in phase and therefore give rise to good coherence. Coherence in a SAR interferogram is not measured, but estimated.

Visualization of Sentinel-1 Coherence Images and Interpretation

The factors likely to cause a change in surface geometry in our study area are mainly sand and vegetation movements and human activities such as livestock passage. These changes cause a loss of coherence and correspond to well defined black areas on the Sentinel-1A coherence images. Figures 12 and 15 show the coherence images obtained from the Sentinel-1 pairs of November 2017 and the Sentinel-1 pairs of May 2015.We can already notice that the majority of the surface are characterized by a good coherence because more than 50 % of pixels has a coherence superior to 0.53 for 2015 and more than 50% of pixels have a coherence greater than 0.83 for 2017.

Table2. *Key for interpreting the color composite of the coherence image and modules of images 1 and 2 in RGB.*

	Level of coherence	Level of amplitude	Interpretation
Black	low	Low	Surface change in 12 days, low roughness or radar wave penetration in a dry environment.
Blue	low	High	Surface change in 12 days, high roughness
Green	low	High	Surface change in 12 days, high roughness
Red	High	Low	Unchanged surface in 12 days, low roughness or penetration of the radar wave in a dry environment
White	High	High	Unchanged surface in 12 days, high roughness

To quickly interpret and differentiate the types of changes, we also exploited the amplitude information by making a colorful composition from the coherence image and modules of the Sentinel-1A images of May 03, 2015 and Sentinel-1A of May 15, 2015 to which we assign the red, green and blue color respectively.

The changes detected (Fig 9, 10, 11) using the coherence image and modules of the Sentinel-1A images are defined as follows:

- Surface change with low roughness (Black): Hassan Addakhil dam retention surface
- Surface change with penetration of the radar wave in a dry environment (Black): zones of silting Zaouiat Aoufous, Yerdi and Jorf.
- Surface change with high roughness (in Blue): these are areas of rock landslides on the slopes.
- Surface change with high roughness (in green): these are high vegetation areas (canopy of trees in the palm grove).
- Stable surface with low roughness or penetration of the radar wave in a dry medium (Red): the reg or desert.

- Stable white surface: metal structures (Errachidia Market cover, ACIMA and parking).

Note that interpreting images is not always easy and that knowledge of the field is always necessary to validate these analyses.

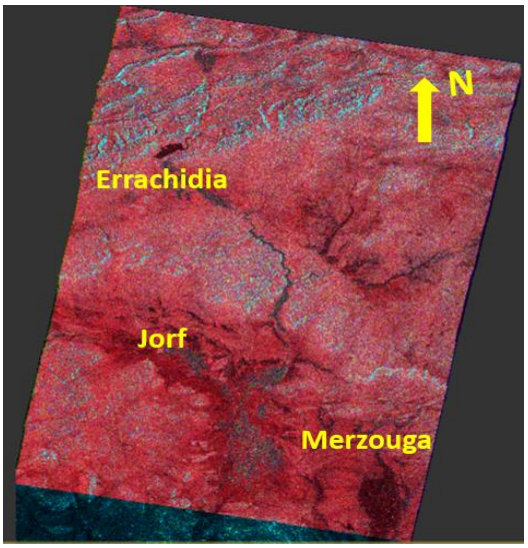

Figure15. *Color composite of coh2015, mod$_1$ 2015 and mod$_2$ 2015 in RGB*

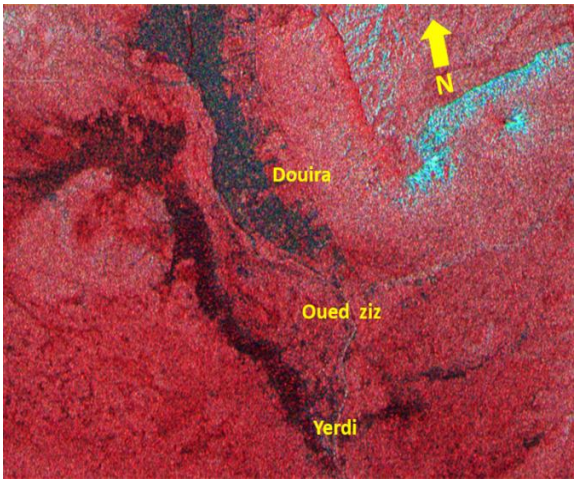

Figure16. *Zoom on Yerdi dunes and Douira palm grove*

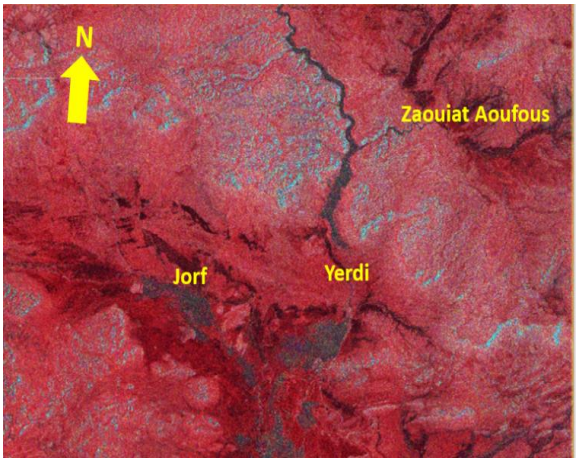

Figure17. *Silting in the study area*

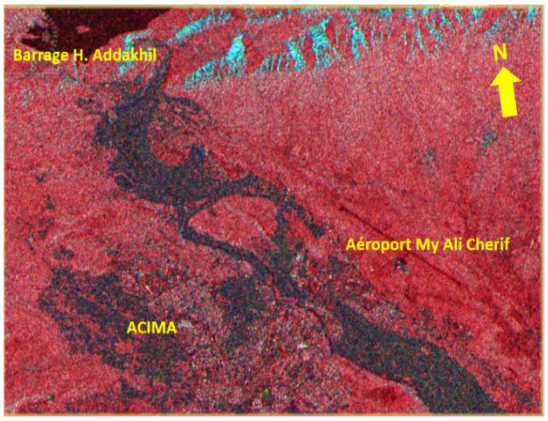

Figure18. *Zooming in on the city of Errachidia with a clear appearance of the Airport runway*

This technique has already been used successfully in Niger, and in Mauritania using ERS1 and ERS2 data (Bodart et al. 2010;Bodart and Ozer 2007). In this way, a simple visual analysis is effective in interpreting the nature of the changes. This image superposition is made possible by the coregistration of all images of the same track. Table 1 provides a summary color interpretative key on the color composition and Figure 6 shows the color composition obtained from the pairs of May 2015 Sentinel-1.

For a sandy area, this loss of coherence should be explained by a windy episode causing a sand movement or by the penetration of the Radar wave into a dry environment. Thus, the coherence image provides original and unique information relative to traditional optical and radar satellite images.

An optical image such as the Lands at image generally identifies the structure of the dunes but does not provide information on surface dynamics and does not identify the limits of the active dunes and the movable sandy sails, especially if the soil properties are very similar (Liu et al. 2001). As for the radar image, it tells us about the roughness and physical properties of the ground but not about the mobility of sand. Consistency therefore seems to be a very good tool for mapping dune activity, as well as for tracking dune movements and silting.

Monitoring and Detecting Change

Evaluation of Sentinel-1A Coherence

We are observing a decrease in the average coherence for pairs the May 2015 compared to the average coherence for pairs the November 2017 because our area is characterized by a low temporal coherence at the level of the moving dunes that make up a large part of the scene.

Table3. *Statistics on Sentinel-1A coherence images.*

Dates	Track	Base (m)	γtheorique	γaverage	γaverage / γtheorique
03 and 15 May 2015	81	-191.79	0.981	0.579	0.590
12 and 24 November 2017	81	-46.16	0.995	0.876	0.880

It was noted that the estimated average consistency in November 2017 is higher than May 2015. However, theoretical coherence is even better in November 2017 than in May 2015. The lower ratio in May 2015 therefore results from a much weaker temporal consistency at this date than in November 2015. This shows that it is crucial to take into account the effect of spatial decorrelation in order to properly compare the results. The analysis of histograms (Fig20 and 21) also highlights the majority of pixels with low coherence is well marked in May 2015 compared to November 2017 (90% of pixels with γ 0.73 in May 2015 and 90% of pixels with γ 0.93 in November 2017). In the Errachidia region a maximum proportion of effective winds are remarkable at the end of the dry season (March-April-May).The fall in interferometric coherence observed during the month of May is explained by the increase in wind activity recorded during this period; which corresponds to the impacts of climatic hazards (soil humidity and wind erosion).

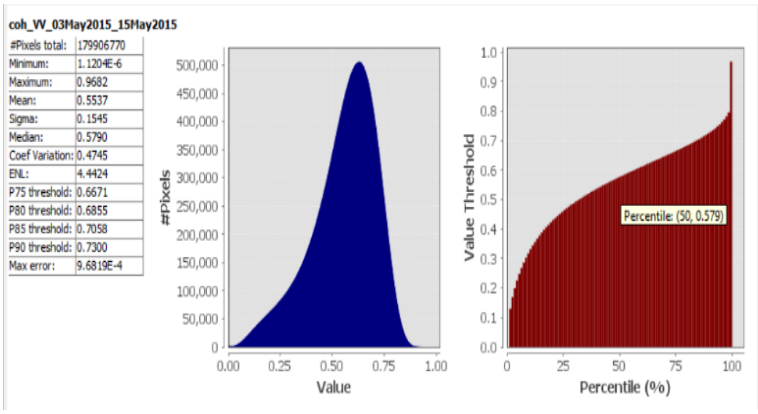

Figure19. *histogram of coherence May2015*

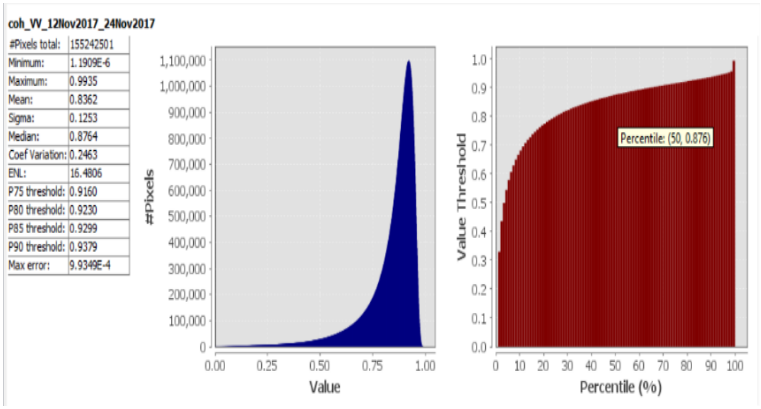

Figure20. *histogram of coherence November 2015*

RGB Combination

Each image of coherence gives us the position of the active dunes. The superposition by means of a colorful composition of two images of Sentinel-1A coherence acquired on different dates could thus illustrate a possible migration of the dunes in the interval between these two dates. For example, for Track 81, the colorful composition, the 2015 coherence image (coh2015) in red, the 2017 coherence image (coh2017) in green, and the master image module ($mod_1$2015) in blue, allows us to detect in green what is moving in May 2015 but not in November 2017, in red what is moving in November 2017 but not in May 2015, in black what is moving on both dates, in blue areas of low coherence but not sand (these are slides) and, finally, in yellow, areas of high coherence but low amplitude. The migration of a "Barkhane", for example, should appear as a black spot with a green wind limit and a red leeward limit.

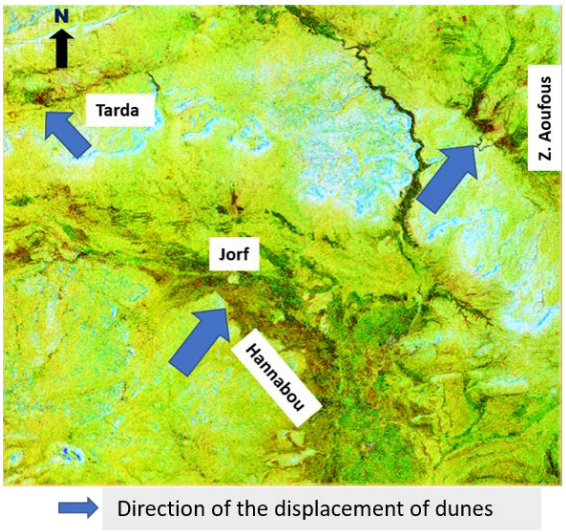

Figure21. *Color Composite RVB= Coh2015_ coh2017_mod*$_1$*2015*

The color composite inspection enables us to find out where sand dunes movements occurred. Figure 22 shows an excerpt from this composition, which shows the increase in sand from 2015 to 2017. In addition, the direction of progress seems to correspond to two privileged directions: the direction of Chergui which blows in the dry season from South-East to North-West (Tarda) and the direction of Saheli which blows from South-West to North-East (Hannabou Jorf and Zaouiat Aoufous).

The same methodology for detecting active dunes was applied successfully in another Sahelian region in Mauritania and on the northern border of the Sahara Desert, in Southern Morocco (Draa valley) (Gassani, J.2004;Ozer, A., et al. 2002, Bodart, C., et al. 2005).

Discussion and Conclusions

The information of interferometric coherence is original and unique with regard to the traditional satellite data. By offering a measure of the dynamics and the changes of surface which take place between both of the pair interferometric acquisitions. Combined with the images of amplitude, the images of coherence obtained from the images Sentinel1A in twelve days apart available on the southeast of Morocco allowed to detect mobile sands.

Then, the temporal analysis of the interferometric coherence was able to highlight the extension of active sandy zones in time. These first visual results are already innovative. Indeed, the only work using coherence images in an arid area (Liu et al. 2001) failed in their attempt to detect dune migration. These authors used multi-temporal coherence ERS 1/2 images of 35, 350 and 385 days to detect changes in an arid area of the Sahara in Algeria. Indeed, the Algerian Sahara, where the soil is composed of bare, vegetative rocky surface and maintains good coherence at 35, 350 and 385 days (Bodart et al.2010).

The Sentinel1A images at 12 days apart therefore seem very interesting for the mapping and study of the dune sands dynamics by interferometric coherence. These sentinel images allowed us to calculate values of coherence whose great utility for dune mapping was demonstrated.

Bibliographie

[1] **Alessandro Ferretti et al., 2007.** In SAR Principles: Guidelines for SAR Interferometry Processing and Interpretation (TM-19)

[2] **Bodart, C., Gassani, J., Salmon, M. & Ozer, A. (2005).** Contribution of SAR interferometry (from ERS1/2) in the study of aeolian transport processes: the cases of Niger, Mauritania and Morocco. Proceedings of 'Fringe 2005 Workshop' (Eds. H. Lacoste), ESA SP-610 (CD-ROM), ESA Publication Division, European Space Agency, Noordwijk, The Netherlands.

[3] **Bodart, C. et Ozer, A., 2007.**The use of SAR interferometric coherence images to study sandy desertification in southeast Niger: preliminary results. ESA Symposium 2007, Montreux, Suisse, ESA, 6p.

[4] **Bodart, C et al., 2010.**Suivi de l'activité des dunes au Niger au moyen de la cohérence interférométrique ERS 1/2. BSGLg, 54, 2010, 123-136

[5] **De Zan F. and Monti Guarnieri A. 2006.**"TOPSAR: Terrain observation by progressive scans," IEEE Trans. Geosciences. Remote Sensing, vol. 44, no. 9, pp. 2352–2360

[6] **Elkharki, O et al., 2016.**Cours de l'interférométrie Radar Faculté des sciences et Technique Tanger Maroc.

[7] **ESA, 2007.** In SAR principles: Guidelines for SAR interferometry processing and interpretation. Noordwijk, The Netherlands, ESA Publication, ESTEC, 232p.

[8] **European Space Agency, 2016** Sentinel-1 Toolbox: TOPS Interferometry Tutorial

[9] **Farkas, P., Hevér, R., Grenerczy, G., 2015.** Geodetic integration of Sentinel-1A IW data using PS In SAR in Hungary. EGU General Assembly Conference Abstracts (p. 13483).

[10] **Gassani, J. (2004).** Apport de la télédétection à l'analyse et à la gestion des risques naturels sur lazone du lac d'Aleg (Brakna, Mauritanie), Master Dissertation, Faculté des Sciences, University of Liège.

[11] **Hervé Rivano, 2014** Modélisation et optimisation du partage de ressources dans les réseaux radio multi-sauts. Réseaux et télécommunications [cs.NI]. INSA Lyon.

[12] **Liu, J. G., et al., 2001.**Land surface change detection in a desert area in Algeria using multi-temporal ERS SAR coherence images. International Journal of Remote Sensing, 22(13), 2463-2477.

[13] **Nestor YagueM.et al. 2016.**Interferometric Processing of Sentinel-1 TOPS Data. IEEE Transactions on Geoscience and Remote Sensing, Vol. 54, No.4

[14] **Ozer, A., et al. 2002.**Etude par télédétection de l'ensablement dans la province de Ouarzazate, Maroc, Project report, Liège.

[15] **Santoro, M. et al., 2007.** Properties of ERS 1/2 in the Siberian boreal forest and implications for stem volume retrieval. Remote Sensing of Environment, 106, 154-172.

[16] **Zebker, H. A. et Villasenor, J., 1992.** Decorrelation in interferometric radar echoes. I.E.E.E. Transactions on Geosciences and Remote Sensing, 30(5), 950-959.

WEB REFERENCES

[1] https://scihub.copernicus.eu/dhus/#/home.(accessed 15 December 2017)

[2] https://earth.esa.int/web/guest/eo-education-and-training/sar-basics-snap-course/concepts (accessed 10 November 2017)

Citation: *Mohamed ABBA, Ali ESSAHLAOUI, Omar ELKHARKI,Jamila MECHBOUH,."The Use of Interferometric Coherence of Sentinel-1a Images to Study Silting in South-East Morocco". Annals of Ecology and Environmental Science 3(2), pp.37- 49*